Morphologic evolution of recent small sub-cortical infarcts and adjacent white matter in the basal ganglia in a Chinese cohort

Sha-Sha Wang[1], Sen Wei[2], Bo Song[1], Yu-Ming Xu[1]

[1]Department of Neurology, the First Affiliated Hospital of Zhengzhou University, Zhengzhou, Henan 450052, China;
[2]Department of Neurological Intervention, the First Affiliated Hospital of Zhengzhou University, Zhengzhou, Henan 450052, China.

Abstract

Background: Data on the evolution of recent small sub-cortical infarcts are limited, especially in the Chinese. Previous studies have reported a large heterogeneity in cavitation and infarct location; therefore, the present study assessed the morphology of small sub-cortical infarcts in the basal ganglia in a Chinese cohort.

Methods: Patients who had experienced a recent, single, small sub-cortical infarct in the basal ganglia and received at least one follow-up magnetic resonance imaging (MRI) scan were retrospectively identified from January 2014 to June 2018. Time to follow-up imaging, baseline infarct size, vascular risk factors, and other clinical data, as well as the morphologic changes of the index infarct and surrounding white matter were recorded. Demographic, clinical and MRI characteristics were respectively compared among three groups (white matter hyper-intensitie [WMH] *vs*. cavitation *vs*. absent) and between with and without new WMH formation groups. In addition, logistic regression analyses were performed in investigating the determinate independent predictors for new WMH formation.

Results: Seventy-eight subjects were included with a median follow-up time of 304 days (range: 124–552 days). We found a significant reduction in infarct size at follow-up: 46 of 78 (59.0%) infarctions showed some degree of cavitation, 19 of 78 (24.4%) index lesions resembled non-cavitated WMH, and 13 of 78 (16.7%) infarcts had disappeared at follow-up MRI. No factors were found to be associated with differential outcomes of the infarcts. In addition, 8 of 78 (10.3%) patients demonstrated new WMH formation surrounding the index infarct; white matter progression (odds ratio = 15.95, 95% confidence interval = 1.65–153.99; $P = 0.017$) was an independent risk factor of new WMH formation.

Conclusions: More than half of the small sub-cortical infarcts in the basal ganglia progressed to cavities, demonstrating that these infarcts can be reduced and go undetected. The presence of new WMH around the infarct may be indicative of the worsening progression of cerebral small vessel diseases. Additionally, white matter progression is an independent risk factor, which may be a potential therapeutic target.

Keywords: Cerebral small vessel disease; Recent small sub-cortical infarct; Stroke; White matter hyper-intensity

Introduction

Cerebral small vessel disease (CSVD) is a common category of age-related cerebrovascular disease and can lead to clinical, imaging, and pathologic syndromes caused by the varying etiologies affecting the perforating cerebral arterioles, capillaries, and venules.[1] As the population ages, the incidence of CSVD continues to rise. Studies suggest that CSVD is responsible for approximately 20% to 25% of strokes and contributes to the cognitive decline that is the most common vascular cause of dementia, movement disorders, vascular Parkinson syndrome, and other clinical symptoms, which impact the patient's daily quality of life.[1-9] Importantly, CSVD is primarily asymptomatic in early diagnosis and relies on imaging examination, particularly brain magnetic resonance imaging (MRI). Characteristics of CSVD on conventional MRI include recent small sub-cortical infarct (RSSI), white matter hyper-intensities (WMH), lacune, enlarged peri-vascular space (EPVS), cerebral microbleed (CMB), and brain atrophy (BA).[10] Notably, CSVD is present in images for many years before cognitive decline and motor dysfunction are apparent. A more thorough description of the evolution of CSVD characteristics in MRI may improve our understanding of its natural disease course.[11]

Small sub-cortical infarcts increase the risk of stroke, dementia, and motor impairment, and distribution characteristics can

Access this article online

Quick Response Code:

Website: www.cmj.org

DOI: 10.1097/CM9.0000000000001041

Correspondence to: Dr. Yu-Ming Xu, Department of Neurology, the First Affiliated Hospital of Zhengzhou University, No. 1 Jianshe Road, Zhengzhou, Henan 450052, China
E-Mail: xuyuming@zzu.edu.cn

Chinese Medical Journal 2020;133(19)
Received: 30-04-2020 **Edited by:** Xiu-Yuan Hao and Xin Chen

help identify the etiologic mechanisms of stroke and determine prognosis.[12] Additionally, studies have demonstrated that RSSI have different outcomes, form cavities or maintain WMH without obvious cavitation on T2-weighted imaging, are not seen on conventional MRI, and can lead to secondary morphologic changes in peripheral white matter.[10,11,13] Data on the evolution of RSSI are limited, especially in the Chinese population. Research suggests that the progression of RSSI may be due to its location; however, no studies have assessed its location evolution using imaging.[14,15] RSSI often occur in the basal ganglia region and are supported by one small perforating arteriole. In this region, white matter fibers are dense and have crucial functions in the regulation of movement; this is also known as the movement center under the cortex. Therefore, we selected to examine RSSI in the basal ganglia and changes to peripheral white matter, thereby increasing our understanding of CSVD and neurodegeneration, which could assist in further treatment. The aim of the present study was to investigate the evolution of RSSI in the basal ganglia region and the changes of surrounding white matter using conventional MRI. Additionally, we assessed the risk factors of any morphologic changes.

Methods

Ethical approval

The study was conducted in accordance with the *Declaration of Helsinki* and was approved by the Ethics Committee of The First Affiliated Hospital of Zhengzhou University (No. 2010 ky45).

Study population

All patients with a single RSSI in the basal ganglia region admitted to the First Affiliated Hospital of Zhengzhou University from January 2014 to June 2018 were retrospectively reviewed. Only patients who were older than 18 years of age and received a follow-up structural MRI after the index infarct were included. Exclusion criteria were patients with lesions caused by other than CSVD, neurodegenerative disease, epilepsy, brain trauma, brain tumor, and other neurologic diseases; or poor baseline data or image quality.

Clinical data

The following data were collected: age, sex, and vascular risk factors (eg, history of stroke, hypertension, diabetes mellitus, dyslipidemia, coronary artery disease, smoking, and alcohol use). Stroke severity was assessed by the National Institutes of Health Stroke Scale (NIHSS) at admission.

MRI and CSVD scores

MRI at baseline and follow-up was performed using a 3.0 Tesla Discovery MR750 scanner (GE Healthcare, Waukesha, WI, USA). The parameters of MRI examination were as follows: axial T1-weighted imaging (T1WI; repetition time [TR] = 3204 ms; echo time [TE] = 24 ms; field of view [FOV] = 24 cm × 24 cm; matrix = 320 × 256; number of excitations [NEX] = 1), axial T2-weighted imaging (T2WI; TR = 3339 ms; TE = 102 ms; FOV = 24 cm × 24 cm; matrix = 288 × 288; NEX = 1), fluid-attenuated inversion recovery sequences (FLAIR; TR = 8400 ms; TE = 120 ms; FOV = 24 cm × 24 cm; matrix = 256 × 192; NEX = 1), axial diffusion-weighted imaging (DWI; TR = 3500 ms; TE = minimum; B-value = 0 and 1000 s/mm^2; FOV = 24 cm × 24 cm; matrix = 160 × 160; NEX for T2 = 1; NEX = 2). All sequences had a slice thickness of 5 mm and inter-slice gap of 1 mm. The Functool MADC software (GE Medical Systems, Milwaukee, WI, USA) was used to post-process DWI raw data to determine the apparent diffusion coefficient.

Imaging data were reviewed by two neuroradiologic experts who were blinded to the clinical data. All imaging manifestations of CSVD were diagnosed and classified according to the Standards for Reporting Vascular changes on Neuroimaging (STRIVE).[10] RSSI was a round or ovoid lesion with a maximum axial diameter of ≤20 mm, occurred in the past few weeks, and located in the area that is supplied by one perforating arteriole.[10] Baseline and follow-up infarct diameter were measured in three directions in axial DWI or FLAIR imaging, in which we adopted the maximum diameter. Most of the lesions occurred in the centrum semiovale, radiating crown, basal ganglia, or brainstem, which demonstrated a high signal in DWI, low signal in apparent diffusion coefficient, and with or without hyper-intensity in FLAIR and T2WI.[10,11]

The cavity of the index infarct was defined as the appearance of a cerebrospinal fluid (CSF) equivalent lesion on T1WI, FLAIR, and T2WI sequences in the original territory. The outcomes of the RSSI were classified into: absent, differing degrees of cavitation (incompletely or completely), and WMH [Figure 1].[11,14-19] A lacune was defined as a round or ovoid fluid-filled cavity with a diameter of 3 to 15 mm with a similar signal to CSF, following a previous RSSI or hemorrhage in the area supplied by one perforating arteriole, and showed hyper-intensity in T1WI, T2WI and surrounding low signal lacune on FLAIR.[10]

WMH were abnormal signals of variable size in the white matter that satisfied the following characteristics: absence of cavity; hyper-intensity on T2WI or FLAIR; and equal or low signal on T1WI, in which the signal was different from CSF.[10] At least three MRI layers above and below the index small sub-cortical infarct were evaluated to determine the presence of new WMH [Figure 2].[11,13] Deep WMH and peri-ventricular WMH were scored using the Fazekas scale, in which peri-ventricular grade 3 or deep grade 2 to 3 were classified as extensive WMH.[20] WMH progress was assessed using a modified Rotterdam progress scale (≥ 1 point).[11,21]

The peri-vascular space was defined as a fluid-filled space that passes through grey or white matter following a vessel. The diameter of the space was less than 3 mm and spaces appear linear when imaged parallel to the course of the vessel and round or ovoid when imaged perpendicular to the course of the vessel.[10] This signal is similar to CSF in all sequences. Basal ganglia EPVS and centrum semiovale

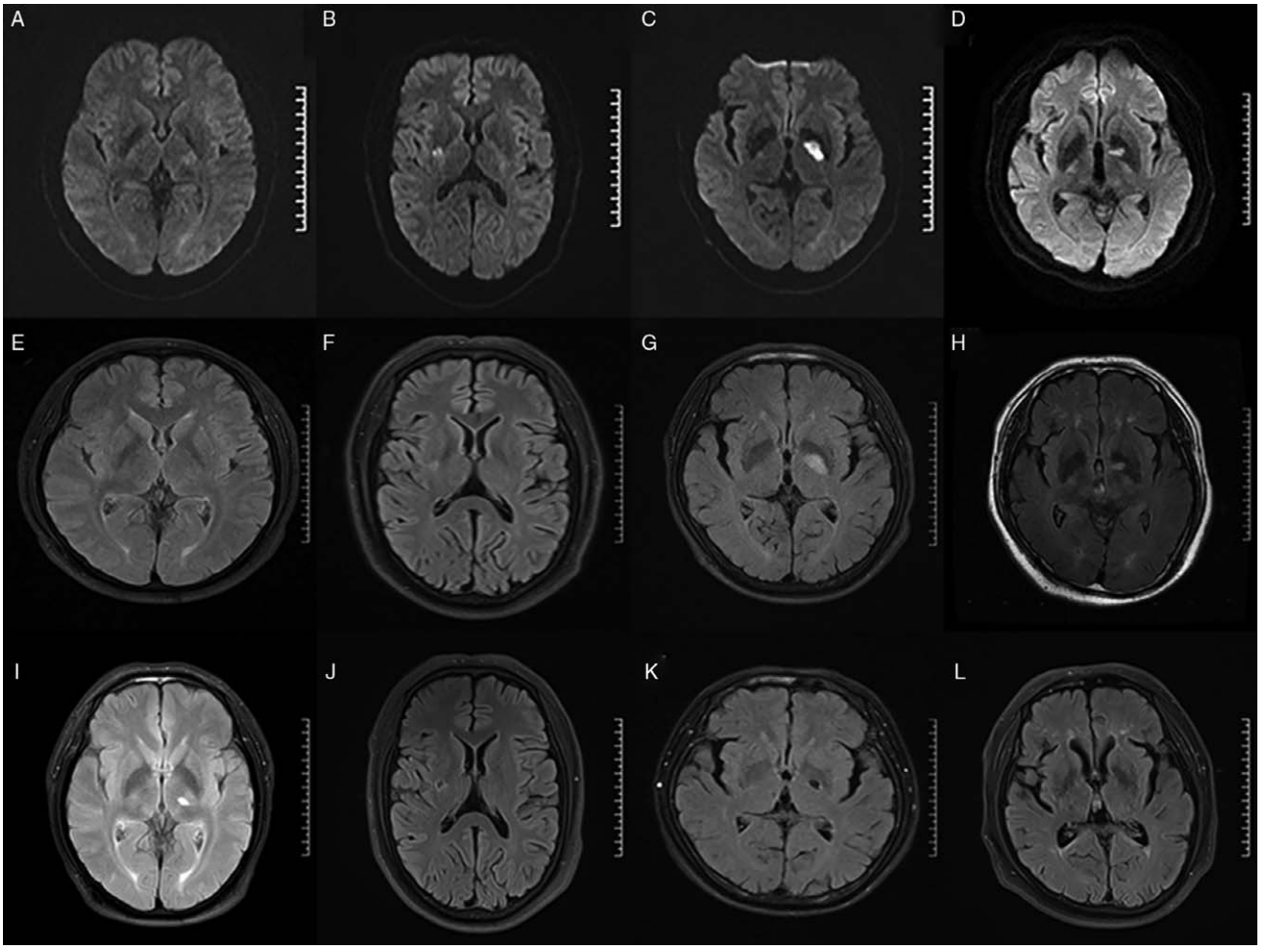

Figure 1: Different outcomes of recent small sub-cortical infarct in the basal ganglia: Diffusion-weighted imaging at baseline (A–D) and fluid-attenuated inversion recovery at baseline (E–H) and follow-up (I–L), respectively. (I) Index infarct resembles white matter hyperintensities. (J) Incomplete cavitation of the index infarct. (K) The lesion completely cavitates. (L) The infarct disappears.

EPVS were assessed for their severity using a 5-point score, where scores of 2–4 were classified as moderate-severe EPVS.[11,22]

Statistical analysis

SPSS statistical software (version 21.0; IBM, Armonk, NY, USA) was used for analysis. The summary statistics were represented by mean ± standard deviation or median (range). Between-group comparisons were made using Student *t* test, analyses of variance, Mann-Whitney *U* test, and Kruskal-Wallis rank test. Categorical variables were represented by percentages and compared with Chi-squared or Fisher exact tests. Finally, we performed logistic regression analyses to determine independent predictors for new WMH formation with age, sex, baseline NIHSS score, baseline DWI diameter, presence of lacunes, and cavity formation in the model. The level of statistical significance was $P \leq 0.05$.

Results

A total of 596 patients with a single RSSI in the basal ganglia region were identified; 78 patients with follow-up imaging were included according to the inclusion and exclusion criteria (mean age: 59.15 ± 13.70 years; female: 23 [29.5%]). The baseline NIHSS score was 1.50 points (range: 1.00–2.00 points). The median follow-up time was 304 days (range: 124–552 days) and 13 patients showed WMH progression on follow-up images. Other baseline features are shown in Table 1. Additionally, the baseline median DWI infarct diameter significantly reduced from 10.40 mm (range: 7.60–12.56 mm) to 7.54 mm (range: 5.31–10.18 mm) at follow-up imaging ($P < 0.001$).

The present study demonstrated that 46 patients (59.0%) with a small sub-cortical infarction in the basal ganglia region had some degree of cavitation, while 18 cases (23.1%) were completely cavitated. Moreover, 19 patients (24.4%) showed WMH at follow-up, indicating no cavities were formed; however, in 13 cases (16.7%), no lesion was seen on follow-up imaging. Univariate analysis and pairwise comparisons among three groups revealed statistically significant differences in follow-up imaging time (WMH *vs.* cavitation *vs.* absent: $P < 0.001$; WMH *vs.* cavitation: $P = 0.027$; WMH *vs.* absent: $P < 0.001$; cavitation *vs.* absent: $P = 0.027$) [Table 1]. With longer follow-up imaging times, infarcts were more likely to cavitate or disappear. When non-significant variables from the univariate analysis were included in multivariate logistic regression analysis, no patient-related, stroke-related, or imaging-related variables

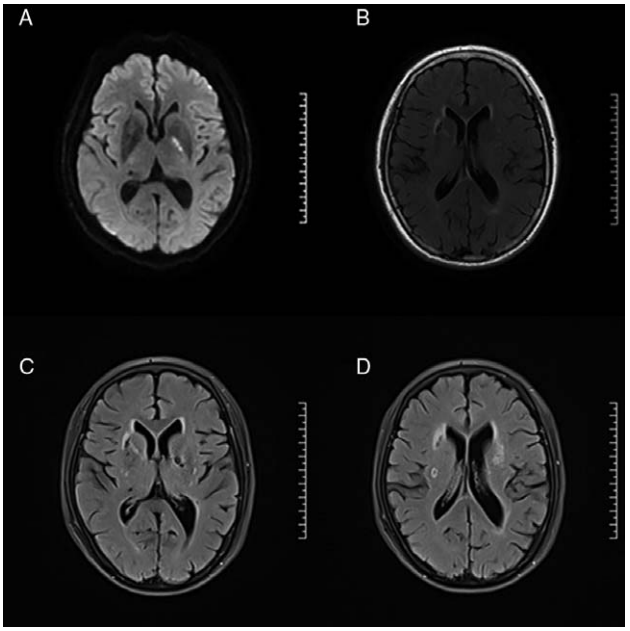

Figure 2: Occurrence of new WMH adjacent to the index infarct. (A) Diffusion-weighted imaging at baseline of RSSI in the basal ganglia. (B) Fluid-attenuated inversion recovery image at baseline surrounding the index infarct. (C) At follow-up, the lesion formed a cavity. (D) At follow-up, new WMH can be seen surrounding the index infarct. WMH: White matter hyper-intensities; RSSI: Recent small sub-cortical infarct.

were found to be associated with imaging outcomes of RSSI in the basal ganglia region after controlling for age and sex.

On follow-up imaging, eight patients (10.3%) demonstrated that new WMH were formed in the area adjacent to the infarct, which was independent of diffuse WMH. Univariate analysis showed that there were no statistically significant differences in age, sex, vascular risk factors, baseline imaging data, and follow-up time between the two groups. WMH progression ($P = 0.030$) and cavity formation ($P = 0.035$) showed statistically significant differences between the two groups [Table 2]. In the multivariate logistic regression analysis, it was found that WMH progression (odds ratio = 15.95, 95% confidence interval = 1.65–153.99; $P = 0.017$) was an independent risk factor for the formation of new WMH in the area adjacent to the RSSI in the basal ganglia region after adjusting for age, sex, baseline NIHSS score, baseline DWI diameter, presence of lacunes, and cavity formation.

Discussion

The present study found that the size of the infarct was reduced by nearly 30% on follow-up imaging and more than half of the patients had some degree of cavitation. Furthermore, approximately 10% of patients presented a new WMH in the area adjacent to the infarct on follow-up and WMH progression was associated with the occurrence of new WMH.

Previous studies have examined infarct size at follow-up imaging and found that the initial infarct was reduced, which is consistent with our present study. This may be related to tissue loss, an ex-vacuo effect in old lesions, and swelling in new lesions.[10,15-17] Varying studies have reported the incidence of cavity formation from 28% to 94%.[11,15-19] Moreau *et al*[14] and Zhang et al[15] found that infarcts at different locations had different outcomes, with a lower incidence of cavitation in the basal ganglia. In the present study, we found that 59.0% of the patients with RSSI in the basal ganglia region presented some degree of cavitation, 24.4% demonstrated a non-cavitated WMH in the index infarct, and 16.7% had disappeared in the follow-up imaging. The heterogeneity of the different outcomes in the index infarct may be related to the differences in the definition of cavitation, the location of infarction, and imaging methods and sequences.

Factors affecting the outcome of infarction remain unclear. Several factors have been reported to be associated with different outcomes of small sub-cortical infarct, including history of hypertension, severity of stroke, longer ischemic times, history of diabetes, WMH, follow-up time, and MRI scanning parameters.[11,15-19] Typically, the morphologic evolution of infarction is related to the follow-up imaging time; however, we found no correlation between the follow-up imaging time and the varying infarct outcomes, which may be due to the small sample size and a large follow-up interval, emphasizing the importance of fixed follow-up times.

We observed the formation of new WMH in the area surrounding the RSSI in 10.3% of patients, which was independent of diffuse WMH and may have different mechanisms. The incidence of the formation of new WMH was relatively low compared with previous studies, which may be related to the location of infarction and the fixed and long follow-up time in previous studies.[11,13] In addition, it was found that WMH progression was an independent risk factor for the formation of new WMH; they may have similar risk factors, although no traditional risk factors were found to be related to the formation of new WMH, such as age and history of hypertension. Wallerian degeneration of white matter fiber tracts is common after large-area cerebral infarction and white matter fiber tracts are dense in the basal ganglia.[23-25] Therefore, cavitation of the basal ganglia region after infarction caused by occlusion of the perforating artery may lead to secondary white matter degeneration or interruption; however, in the present study, we found no association between cavity formation after index infarct and the formation of new WMH, which may be related to the small sample size of new WMH and the non-fixed follow-up time. Infarction cavitation could affect the connectivity of white matter tracts; longitudinal MRI studies of CADASIL patients have shown that small sub-cortical infarcts can affect the integrity of white matter tracts by leading to tract degeneration, which causes the secondary cortical thinning, leading to worse clinical outcomes that affect cognition, motor functions, emotion, and other functions.[26,27] The differing fates of small sub-cortical infarcts in the basal ganglia with dense white matter fiber tracts may also lead to a series of clinical symptoms. The formation of new WMH may be a feature of the deterioration of CSVD found through MRI, and its clinical and prognostic value should be further studied to guide treatment.

Table 1: Demographic, clinical, and MRI characteristics and comparisons among three groups according to outcomes of RSSI.

Items	Total ($n=78$)	WMH ($n=19$)	Cavitation ($n=46$)	Absent ($n=13$)	Statistical values	P
Patient characteristics						
Age (years), mean ± SD	59.15 ± 13.70	58.21 ± 3.42	60.59 ± 1.90	55.46 ± 4.14	0.764*	0.469
Male, *n* (%)	55 (70.5)	13 (68.4)	33 (71.7)	9 (69.2)	0.084†	0.959
Baseline NIHSS score, median (range)	1.50 (1.00–2.00)	2.00 (1.00–2.00)	2.00 (1.00–2.00)	1.00 (0–2.50)	2.346‡	0.309
Vascular risk factors, *n* (%)						
Stroke	12 (15.4)	3 (15.8)	8 (17.4)	1 (7.7)		0.827§
Hypertension	42 (53.8)	9 (47.4)	26 (56.5)	7 (53.8)	0.453†	0.797
Diabetes mellitus	22 (28.2)	6 (31.6)	12 (26.1)	4 (30.8)	0.251†	0.882
Hyperlipidemia	26 (33.3)	5 (26.3)	16 (34.8)	5 (38.5)	0.618†	0.734
Coronary artery disease	11 (14.1)	2 (10.5)	6 (13.0)	3 (23.1)		0.595§
Smoking	26 (33.3)	6 (31.6)	14 (30.4)	6 (46.2)	1.162†	0.559
Alcohol use	13 (16.7)	3 (15.8)	5 (10.9)	5 (38.5)		0.078§
Baseline imaging parameters						
DWI diameter (mm), Median (range)	10.40 (7.60–12.56)	9.78 (7.79–12.52)	11.44 (8.95–13.19)	6.67 (5.67–12.01)	8.197‡	0.017
Presence of lacunes, *n* (%)	52 (66.7)	11 (57.9)	32 (66.7)	9 (69.2)	0.870†	0.647
Extensive PWMH, *n* (%)	9 (11.5)	2 (10.5)	5 (10.9)	2 (15.4)		0.886§
Extensive DWMH, *n* (%)	30 (38.5)	8 (42.1)	16 (34.8)	6 (46.2)	0.695†	0.707
Moderate-extensive BG-EPVS, *n* (%)	17 (21.8)	3 (15.8)	12 (26.1)	2 (15.4)		0.639§
Moderate-extensive CSO-EPVS, *n* (%)	26 (32.1)	6 (31.6)	17 (37.0)	3 (23.1)	0.913†	0.633
Follow-up imaging parameters						
FLAIR diameter (mm), Median (range)	7.54 (5.31–10.18)	8.48 (7.08–9.70)	8.89 (6.86–10.72)	0 (0–0)	32.266‡	<0.001
Follow-up time (days), Median (range)	304 (124–552)	92 (19–335)	304 (159–541)	626 (391–856)	18.262‡	<0.001
WMH progression, *n* (%)	13 (16.7)	3 (15.8)	9 (19.6)	1 (7.7)		0.703§

* Analysis of variance. † Chi-squared test. ‡ Kruskal-Wallis rank test. § Fisher exact test. Extensive PWMH: PWMH Fazekas 3; Extensive DWMH: DWMH Fazekas 2–3; Moderate-extensive BG-EPVS: Grade 2–4; Moderate-extensive CSO-EPVS: Grade 2–4. MRI: Magnetic resonance imaging; RSSI: Recent small sub-cortical infarcts; WMH: White matter hyper-intensities; SD: Standard deviation; NIHSS: National Institutes of Health Stroke Scale; DWI: Diffusion-weighted imaging; PWMH: Peri-ventricular white matter hyper-intensities; DWMH: Deep white matter hyper-intensities; BG-EPVS: Basal ganglia-enlarged peri-vascular space; CSO-EPVS: Centrum semiovale-enlarged peri-vascular space; FLAIR: Fluid-attenuated inversion recovery.

Table 2: Clinical characteristics between subjects with new WMH formation and without new WMH formation.

Items	Absent ($n=70$)	Present ($n=8$)	Statistical values	P
Patient characteristic				
Age (years), mean ± SD	59.21 ± 13.82	58.63 ± 13.48	0.115*	0.909
Male, *n* (%)	50 (71.4)	5 (62.5)	0.013†	0.908
Baseline NIHSS score, median (range)	2.00 (1.25–3.75)	1.00 (0.75–2.00)	195.5‡	0.152
Vascular risk factors, *n* (%)				
Stroke	12 (17.1)	0	0.571†	0.450
Hypertension	37 (52.9)	5 (62.5)	0.021†	0.886
Diabetes mellitus	20 (28.6)	2 (25.0)	0†	1.000
Hyperlipidemia	22 (31.4)	4 (50.0)	0.435†	0.509
Coronary artery disease	11 (15.7)	0	0.454†	0.501
Smoking	24 (34.3)	2 (25.0)	0.017†	0.895
Alcohol use	13 (18.6)	0	0.696†	0.404
Baseline imaging parameters				
DWI diameter (mm), median (range)	11.84 (9.38–13.37)	10.27 (7.34–12.45)	197.500‡	0.174
Presence of lacunes, *n* (%)	44 (62.9)	8 (100)	2.942†	0.086
Extensive PWMH, *n* (%)	9 (12.9)	0	–	0.586
Extensive DWMH, *n* (%)	27 (38.6)	3 (37.5)	0†	1.000
Moderate–extensive BG-EPVS, *n* (%)	14 (20.0)	3 (37.5)	0.468†	0.494
Moderate–extensive CSO-EPVS, *n* (%)	25 (35.7)	1 (3.8)	0.853†	0.356
Follow-up imaging parameters				
Follow-up time (days), median (range)	415 (241–524)	291 (101–596)	222.000‡	0.339
WMH progression, *n* (%)	9 (12.9)	4 (50.0)	4.708†	0.030
Cavitation, *n* (%)	38 (41.3)	8 (100.0)	4.456†	0.035

* Student *t* test. † Chi-squared test. ‡ Mann-Whitney *U* test. Extensive PWMH: PWMH Fazekas 3; Extensive DWMH: DWMH Fazekas 2–3; Moderate-extensive BG-EPVS: Grade 2–4; Moderate-extensive CSO-EPVS: Grade 2–4. WMH: White matter hyper-intensities; SD: Standard deviation; NIHSS: National Institutes of Health Stroke Scale; DWI: Diffusion-weighted imaging; PWMH: Peri-ventricular white matter hyper-intensities; DWMH: Deep white matter hyper-intensities; BG-EPVS: Basal ganglia-enlarged peri-vascular space; CSO-EPVS: Centrum semiovale-enlarged peri-vascular space.

There are notable strengths to the present study. First, both baseline and follow-up MRI were performed using a 3T MRI scan, which was advantageous due to its high spatial resolution and sufficient detection of RSSI and small WMH. Second, all imaging manifestations of CSVD were diagnosed and classified according to STRIVE. Furthermore, we specifically explored the morphologic changes of small subcortical infarcts only in the basal ganglia region, which is more likely to elicit small heterogeneous results. However, our present study also has some limitations. This is a retrospective study with selection bias, a small sample size, and a large follow-up interval. There were many factors that were not considered and the effect of morphologic evolution on cognitive motor function was not evaluated. Going forward, we can increase the sample size, preemptively fix the follow-up time, and prospectively explore the morphologic evolution of infarction at different locations, as well as assess their clinical and prognostic values, which may be a potential therapeutic target.

The present study found cavitation of varying degrees and secondary changes in the surrounding white matter of RSSI in the basal ganglia region, and that the cavitation was a dynamic process with a reduction size or even disappeared over time. The formation of new WMH adjacent to the infarction may be a feature of the deterioration of CSVD, and white matter progression is considered an independent risk factor.

Conflicts of interest

None.

References

1. Wardlaw JM, Smith C, Dichgans M. Mechanisms of sporadic cerebral small vessel disease: insights from neuroimaging. Lancet Neurol 2013;12:483–497. doi: 10.1016/s1474-4422(13)70060-7.
2. de Laat KF, Tuladhar AM, van Norden AG, Norris DG, Zwiers MP, de Leeuw FE. Loss of white matter integrity is associated with gait disorders in cerebral small vessel disease. Brain 2011;134:73–83. doi: 10.1093/brain/awq343.
3. de Laat KF, van Norden AG, Gons RA, van Uden IW, Zwiers MP, Bloem BR, *et al*. Cerebral white matter lesions and lacunar infarcts contribute to the presence of mild parkinsonian signs. Stroke 2012;43:2574–2579. doi: 10.1161/STROKEAHA.112.657130.
4. Hatate J, Miwa K, Matsumoto M, Sasaki T, Yagita Y, Sakaguchi M, *et al*. Association between cerebral small vessel diseases and mild parkinsonian signs in the elderly with vascular risk factors. Parkinsonism Relat Disord 2016;26:29–34. doi: 10.1016/j.parkreldis.2016.02.011.
5. Pavlovic AM, Pekmezovic T, Tomic G, Trajkovic JZ, Sternic N. Baseline predictors of cognitive decline in patients with cerebral small vessel disease. J Alzheimers Dis 2014;42:S37–43. doi: 10.3233/JAD-132606.
6. Schneider AT, Kissela B, Woo D, Kleindorfer D, Alwell K, Miller R, *et al*. Ischemic stroke subtypes: a population-based study of incidence rates among blacks and whites. Stroke 2004;35:1552–1556. doi: 10.1161/01.STR.0000129335.28301.f5.
7. Srikanth V, Phan TG, Chen J, Beare R, Stapleton JM, Reutens DC. The location of white matter lesions and gait–a voxel-based study. Ann Neurol 2010;67:265–269. doi: 10.1002/ana.21826.
8. van der Flier WM, van Straaten EC, Barkhof F, Verdelho A, Madureira S, Pantoni L, *et al*. Small vessel disease and general cognitive function in nondisabled elderly: the LADIS study. Stroke 2005;36:2116–2120. doi: 10.1161/01.STR.0000179092.59909.42.
9. Liu Y, Dong YH, Lyu PY, Chen WH, Li R. Hypertension-induced cerebral small vessel disease leading to cognitive impairment. Chin Med J 2018;131:615–619. doi: 10.4103/0366-6999.226069.
10. Wardlaw JM, Smith EE, Biessels GJ, Cordonnier C, Fazekas F, Frayne R, *et al*. Neuroimaging standards for research into small vessel disease and its contribution to ageing and neurodegeneration. Lancet Neurol 2013;12:822–838. doi: 10.1016/s1474-4422(13)70124-8.
11. Loos CMJ, Makin SDJ, Staals J, Dennis MS, van Oostenbrugge RJ, Wardlaw JM. Long-term morphological changes of symptomatic lacunar infarcts and surrounding white matter on structural magnetic resonance imaging. Stroke 2018;49:1183–1188. doi: 10.1161/STROKEAHA.117.020495.
12. Eppinger S, Gattringer T, Nachbaur L, Fandler S, Pirpamer L, Ropele S, *et al*. Are morphologic features of recent small subcortical infarcts related to specific etiologic aspects? Ther Adv Neurol Disord 2019;12:1756286419835716. doi: 10.1177/1756286419835716.
13. Loos CMJ, van Oostenbrugge RJ, Staals J. The appearance of a new white matter lesion adjacent to the old infarct in first-ever Lacunar stroke patients: a two-year follow-up study with MRI. Cerebrovasc Dis 2012;34:443–445. doi: 10.1159/000344003.
14. Moreau F, Patel S, Lauzon ML, McCreary CR, Goyal M, Frayne R, *et al*. Cavitation after acute symptomatic lacunar stroke depends on time, location, and MRI sequence. Stroke 2012;43:1837–1842. doi: 10.1161/STROKEAHA.111.647859.
15. Zhang X, Ding L, Yang L, Qin W, Li Y, Li S, *et al*. Relationship between white matter hyperintensities penumbra and cavity formation. Med Sci Monit 2016;22:41–49. doi: 10.12659/msm.896324.
16. Koch S, McClendon MS, Bhatia R. Imaging evolution of acute lacunar infarction: leukoariosis or lacune? Neurology 2011;77:1091–1095. doi: 10.1212/WNL.0b013e31822e1470.
17. Loos CM, Staals J, Wardlaw JM, van Oostenbrugge RJ. Cavitation of deep lacunar infarcts in patients with first-ever lacunar stroke: a 2-year follow-up study with MR. Stroke 2012;43:2245–2247. doi: 10.1161/STROKEAHA.112.660076.
18. Pinter D, Gattringer T, Enzinger C, Seifert-Held T, Kneihsl M, Fandler S, *et al*. Longitudinal MRI dynamics of recent small subcortical infarcts and possible predictors. J Cereb Blood Flow Metab 2019;39:1669–1677. doi: 10.1177/0271678X18775215.
19. Potter GM, Doubal FN, Jackson CA, Chappell FM, Sudlow CL, Dennis MS, *et al*. Counting cavitating lacunes underestimates the burden of lacunar infarction. Stroke 2010;41:267–272. doi: 10.1161/STROKEAHA.109.566307.
20. van Straaten EC, Fazekas F, Rostrup E, Scheltens P, Schmidt R, Pantoni L, *et al*. Impact of white matter hyperintensities scoring method on correlations with clinical data: the LADIS study. Stroke 2006;37:836–840. doi: 10.1161/01.STR.0000202585.26325.74.
21. Gouw AA, van der Flier WM, Fazekas F, van Straaten EC, Pantoni L, Poggesi A, *et al*. Progression of white matter hyperintensities and incidence of new lacunes over a 3-year period: the leukoaraiosis and disability study. Stroke 2008;39:1414–1420. doi: 10.1161/STROKEAHA.107.498535.
22. Doubal FN, MacLullich AM, Ferguson KJ, Dennis MS, Wardlaw JM. Enlarged perivascular spaces on MRI are a feature of cerebral small vessel disease. Stroke 2010;41:450–454. doi: 10.1161/STROKEAHA.109.564914.
23. Matsusue E, Sugihara S, Fujii S, Kinoshita T, Ohama E, Ogawa T. Wallerian degeneration of the corticospinal tracts: postmortem MR-pathologic correlations. Acta Radiol 2007;48:690–694. doi: 10.1080/02841850701342112.
24. Thomalla G, Glauche V, Weiller C, Rother J. Time course of wallerian degeneration after ischaemic stroke revealed by diffusion tensor imaging. J Neurol Neurosurg Psychiatry 2005;76:266–268. doi: 10.1136/jnnp.2004.046375.
25. Zhang J, Zhang Y, Xing S, Liang Z, Zeng J. Secondary neurodegeneration in remote regions after focal cerebral infarction: a new target for stroke management? Stroke 2012;43:1700–1705. doi: 10.1161/STROKEAHA.111.632448.
26. Duering M, Righart R, Csanadi E, Jouvent E, Herve D, Chabriat H, *et al*. Incident subcortical infarcts induce focal thinning in connected cortical regions. Neurology 2012;79:2025–2028. doi: 10.1212/WNL.0b013e3182749f39.
27. Jouvent E, Mangin JF, Porcher R, Viswanathan A, O'Sullivan M, Guichard JP, *et al*. Cortical changes in cerebral small vessel diseases: a 3D MRI study of cortical morphology in CADASIL. Brain 2008;131:2201–2208. doi: 10.1093/brain/awn129.

How to cite this article: Wang SS, Wei S, Song B, Xu YM. Morphologic evolution of recent small sub-cortical infarcts and adjacent white matter in the basal ganglia in a Chinese cohort. Chin Med J 2020;133:2302–2307. doi: 10.1097/CM9.0000000000001041